

General Disclaimer

One or more of the Following Statements may affect this Document

- This document has been reproduced from the best copy furnished by the organizational source. It is being released in the interest of making available as much information as possible.
- This document may contain data, which exceeds the sheet parameters. It was furnished in this condition by the organizational source and is the best copy available.
- This document may contain tone-on-tone or color graphs, charts and/or pictures, which have been reproduced in black and white.
- This document is paginated as submitted by the original source.
- Portions of this document are not fully legible due to the historical nature of some of the material. However, it is the best reproduction available from the original submission.

SATELLITE TO SATELLITE TRACKING
ERROR ANALYSIS STUDIES
AND
DATA PROCESSING

Prepared For
NATIONAL AERONAUTICS AND SPACE ADMINISTRATION
Goddard Space Flight Center
Greenbelt, Maryland

CONTRACT ~~NAS 5-11999~~
Task Assignment 418

OCTOBER 1975

(NASA-CR-144832) SATELLITE TO SATELLITE
TRACKING ERROR ANALYSIS STUDIES AND DATA
PROCESSING (Computer Sciences Corp.) 32 p
HC A03/MF A01 CSCL 22A



Unclas

G3/15 50933

CSC
COMPUTER SCIENCES CORPORATION

SATELLITE TO SATELLITE TRACKING
ERROR ANALYSIS STUDIES
AND DATA PROCESSING

Prepared for
GODDARD SPACE FLIGHT CENTER

by
COMPUTER SCIENCES CORPORATION

Under
Contract NAS 5-11999
Task Assignment 418

Prepared by:

Approved by:

C. L. Ayres 8/25/75
C. L. Ayres Date

G. P. Spears 8/25/75
G. P. Spears Date

Dr. G. Rosenblatt 6/25/75
Dr. G. Rosenblatt Date

James O. Cappellari Jr. for 10/13/75
W. E. Wagner Date

ABSTRACT

This Technical Memorandum is the final deliverable item required by Task Assignment 418, Tracker Calibration Using SST Data. It presents the results of all studies conducted under this task which were not documented previously in Technical Memorandum CSC/TM-75/6110. The error analysis studies examine the effects of placing the target satellite in an orbit nearly coplanar with the relay satellite and of data span length on the accuracy with which the satellite states can be recovered. An analysis of error models using actual SST data spans is also included.

TABLE OF CONTENTS

<u>Section 1 - Introduction</u>	1-1
<u>Section 2 - Error Analysis Studies</u>	2-1
2.1 Nearly Coplanar Orbits	2-1
2.2 Simulated Trilateration Data	2-6
2.3 Real GEOS-3 Data	2-11
<u>Section 3 - Differential Correction Processing of Real SST Data</u>	3-1
<u>Appendix A - Mathematical Method Used in Error Analyses</u>	
<u>References</u>	

LIST OF ILLUSTRATIONS

Figure

- 2-1 Maximum Uncertainties of Target Satellite Position Due to Consider Parameters as a Function of Relative Inclination Angle Between Orbital Planes of Target and Relay Satellites . . 2-5

LIST OF TABLES

Table

- 2-1 Uncertainties Assumed for the Measurements and for the Consider Parameters 2-3
- 2-2 Target Satellite Uncertainties as a Function of Relative Inclination Angle Between Orbital Planes of Target and Relay Satellites 2-4
- 2-3 Results of Error Analysis Runs Using Simulated Trilateration and SST Data 2-7
- 2-4 Uncertainties Assumed for the Measurements and for the Consider Parameters 2-13
- 2-5 GEOS-3 (Target) and ATS-6 (Relay) State Vector Uncertainties at Epoch, Using Only SST Data 2-15
- 2-6 GEOS-3 (Target) and ATS-6 (Relay) State Vector Uncertainties at Epoch, Using SST Data and ATS-6 Tracking Data 2-16
- 2-7 GEOS-3 (Target) State Vector Uncertainties, Using SST Data and Considering ATS-6 (Relay) State Vector Uncertainties . . . 2-17
- 3-1 GEOS-3 (Target) State Vector Deviations and Uncertainties, Using SST Data 3-2
- 3-2 GEOS-3 (Target) and ATS-6 (Relay) State Vector Deviations and Uncertainties, Using SST Data 3-4

SECTION 1 - INTRODUCTION

Satellite-to-satellite tracking (SST) provides a type of orbit observation not previously used in orbit determination and data analysis. The observation modeling differs from that used in single spacecraft, since it includes the dynamics of two satellite orbits, together with the relative geometrical configuration of the satellites and ground station. Analysis of this type of data requires information on the effect of deviations in one satellite orbit on the solution obtained for the other satellite orbit, and on the influence of other error models on the solutions obtained for both satellites.

The purpose of Task Assignment 418 is to provide support in the analysis of the capability to determine satellite trajectories, system biases, and other parameters using SST data. This memorandum presents the results of all studies conducted under this task which were not documented previously in Technical Memorandum CSC/TM-75/6110. The studies documented in this memorandum include error analyses on simulated and real satellite-to-satellite tracking (SST) data, and differential correction processing of selected spans of the real SST data. Error analysis studies include:

- Examination of the effects of placing the target satellite in an orbit nearly coplanar with the relay satellite
- Examination of the effects of data span length on the accuracy of recovery of either or both state vectors when SST data is supplemented with trilateration tracking data from the relay satellite
- Analysis of errors modeled in the SST formulation using real data from the Applications Technology Satellite-6 (ATS-6) and the Geodynamics Experimental Ocean Satellite-3 (GEOS-3)

These error analysis studies are documented in Section 2. Section 3 presents the results of differential correction processing of selected spans of real SST data to obtain ATS-6 and GEOS-3 state vectors and associated uncertainties.

SECTION 2 - ERROR ANALYSIS STUDIES

2.1 NEARLY COPLANAR ORBITS

The study described in this section was conducted in order to determine the accuracy with which the target satellite orbit can be determined using SST data in the case where the target and the relay satellite orbits are coplanar, or nearly so. This anticipates situations which may arise in the Tracking Data Relay Satellite System (TDRSS), where some of the target satellite orbits are expected to be equatorial. The objective of the study was to determine the minimum relative inclination of the satellite orbits which permits recovery of the target satellite state vector to within a given margin of error.

To that end, 6-hour and 24-hour spans of simulated satellite-to-satellite data were generated by the Navigation Analysis Program (NAP) for each of eight target satellite orbits having different (but small) inclination angles relative to the relay satellite orbital plane. The simulated relay satellite was placed over the Galapagos Islands in a geosynchronous orbit with an inclination of approximately one degree relative to the equator. The companion target satellite orbits were approximately circular with heights of 840 km, periods of approximately 100 minutes, and inclinations relative to the relay satellite orbit of 0.0, 0.25, 0.50, 1.0, 2.0, 3.0, 4.0, and 5.0 degrees. Both range and Doppler data from Rosman were simulated, with a 1-minute separation between the data points.

Starting with a priori state vectors unperturbed from the values with which the data were originally generated, the simulated data were processed by NAP for one iteration in the differential correction mode. The normal matrix computed during the differential correction process and the orbit files generated by the integrator were passed to the NAP covariance analysis program (NAPCOV), which used this information to compute the contributions

to solve-for uncertainties arising from the uncertainties in the consider parameters and to propagate these quantities in time.

The analyses were performed by considering uncertainties in the relay satellite state vector and in several other parameters. The data weights used and the uncertainties assumed for the consider parameters are shown in Table 2-1.

The uncertainties computed for the solve-for parameters were rotated into radial, along-track, and cross-track coordinates (HLC) and propagated through the data span. The largest uncertainties encountered in the propagated span were then tabulated.

Table 2-2 lists the computed uncertainties in the target satellite position (in HLC coordinates) arising from the data noise and from the consider parameters for the various relative inclination angles for both the 6-hour and 24-hour data spans. Note that, for the 6-hour data spans, the radial and along-track uncertainties are insensitive to the relative inclination angle except for zero degrees, where the uncertainties increase by up to 40%. However, the cross-track uncertainties show a very sensitive dependence on the relative inclination angle, becoming very large when the target and relay satellite orbits are precisely coplanar. The sensitivity is demonstrated in Figure 2-1, where the maximum uncertainties due to consider variables are plotted as a function of the relative inclination angle.

The computed uncertainties for the 24-hour spans show a similar behavior. The radial and along-track uncertainties are insensitive to the relative inclination angle, but the cross-track uncertainties increase as the relative inclination angle decreases. Figure 2-1 illustrates that the cross-track uncertainties for the 24-hour spans are smaller and not as sensitive to relative inclination angle as those of the 6-hour spans when the orbits become coplanar.

Table 2-1. Uncertainties Assumed for the Measurements
and for the Consider Parameters

A: Uncertainties in SST Data (Weighting Factors)

Range:	6×10^{-8} sec = 9 meters (one-way)
Doppler:	6×10^{-8} sec = 0.002 Hz

B: Uncertainties in Consider Parameters

Consider satellite position:	100 meters (each component)
Consider satellite velocity:	1 cm/sec (each component)
Rosman station location:	10 meters (each component)
Range bias:	10^{-7} sec = 15 meters (one-way)
Doppler bias:	5×10^{-8} sec = 0.002 Hz
Solar pressure on ATS-6:	10%
C_{00} (coefficient of spherically symmetric component of gravitational field):	2×10^{-6}
C_{20} (coefficient of quadrupole term in gravitational field):	9.2×10^{-9}

Table 2-2. Target Satellite Uncertainties as a Function of Relative Inclination Angle Between Orbital Planes of Target and Relay Satellites

Data Span	Relative Inclination Angle (deg)	Max. Uncertainties Due to Noise			Max. Uncertainties Due to Consider Parameters			Significant Consider Parameters
		H	L	C	H	L	C	
6-Hour	0	0.08	0.25	717.6	51.4	255.5	201000	Relay Satellite State Vector and Gravitational Constant
	0.25	0.06	0.20	21.7	44.4	179.7	4440	
	0.5	0.06	0.20	10.7	44.3	179.3	2208	
	1.0	0.06	0.20	5.02	44.3	178.7	1038	
	2.0	0.06	0.20	2.67	44.3	179.0	550.6	
	3.0	0.06	0.20	1.77	44.6	180.0	374.5	
	4.0	0.06	0.20	1.33	44.7	180.0	282.2	
	5.0	0.06	0.20	1.06	44.7	180.0	227.2	
24-Hour	0	0.018	0.064	14.94	35.2	636.7	5136	Relay Satellite State Vector and Gravitational Constant
	0.25	0.017	0.064	6.04	36.0	637.2	1015	
	0.5	0.017	0.064	3.28	35.9	636.6	492.4	
	1.0	0.017	0.064	1.62	35.5	635.5	282.0	
	2.0	0.017	0.064	0.85	35.7	636.0	134.2	
	3.0	0.017	0.064	0.57	35.9	636.1	93.3	
	4.0	0.017	0.064	0.42	35.9	635.8	80.6	
	5.0	0.017	0.064	0.34	36.0	635.6	73.0	

Notes:

- 1) Results are tabulated for both 6-hour and 24-hour data spans.
- 2) Units for radial (H), along-track (L), and cross-track (C) uncertainties are meters.

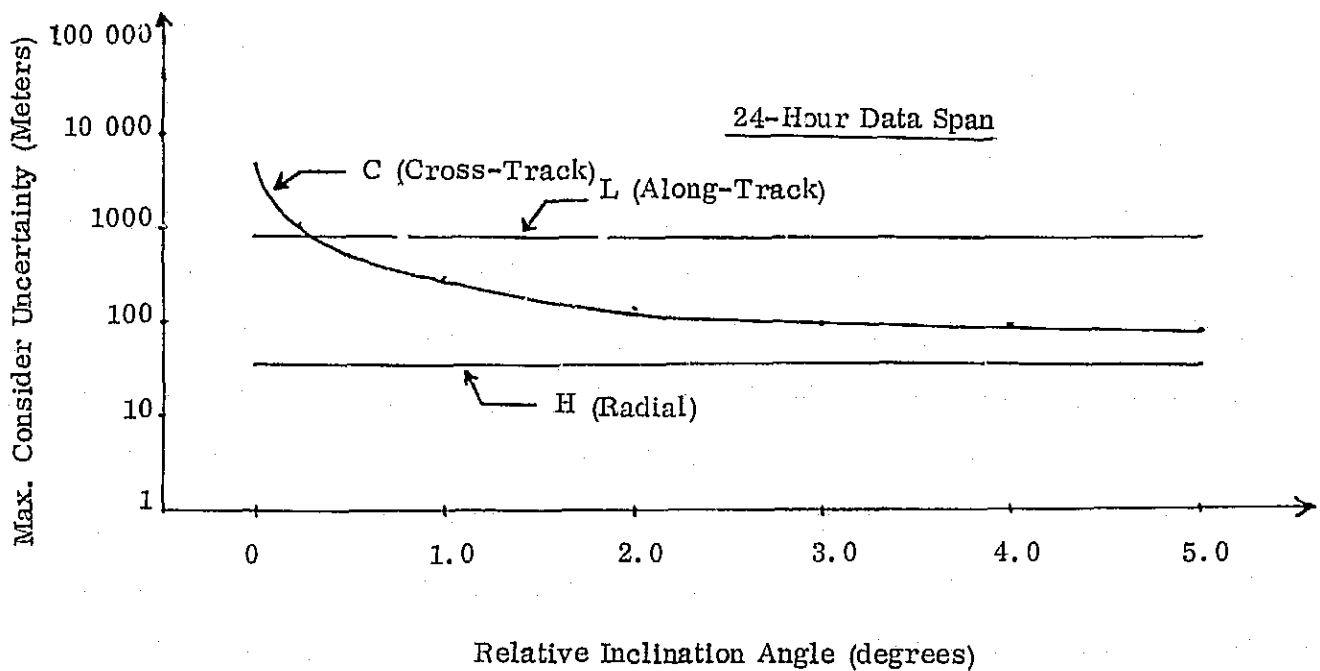
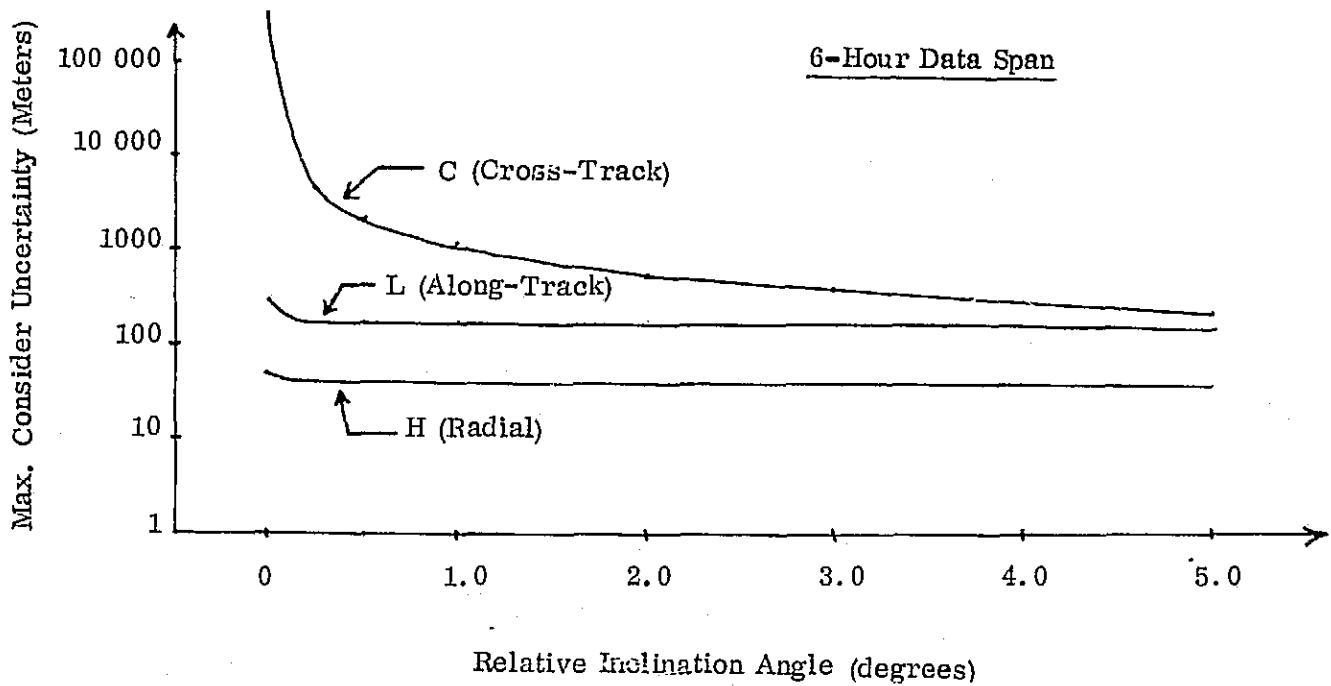


Figure 2-1 Maximum Uncertainties of Target Satellite Position Due to Consider Parameters as a Function of Relative Inclination Angle Between Orbital Planes of Target and Relay Satellites

In practice, it is highly unlikely that the target and the relay satellite orbits will be precisely coplanar. However, the results presented here demonstrate the great advantage to be obtained by ensuring that the relative inclination angle is greater than one or two degrees.

2.2 SIMULATED TRILATERATION DATA

Error analysis runs were made adding simulated trilateration data to the SST data used for the differential correction runs described previously in Section 2 and Tables 2-2(a) and (b) of Reference 1. The data consisted of 12 hours of GEOS-3 SST data taken from Rosman via the ATS-6 relay satellite, augmented by equal quantities of coherent-mode data and data relayed by ground transponders located at Mojave and GSFC. The coherent-mode and ground-transponder data were taken while GEOS-3 was behind the Earth. Error analysis runs were made to include 6 hours and 12 hours of this data, thus corresponding to the earlier differential correction runs. Analysis was performed in three configurations:

- a) Solve for the GEOS-3 state vector only, consider uncertainties* in the ATS-6 state vector and in several other parameters
- b) Solve for the ATS-6 state vector only, consider uncertainties* in the GEOS-3 state vector and in several other parameters
- c) Solve for both the GEOS-3 and the ATS-6 state vectors, consider uncertainties* in several other parameters

For runs in configurations (a) and (b) above, the computed uncertainties in the solve-for parameters were rotated to radial, along-track, and cross-track (HLC) coordinates and propagated forward through the data span. The results listed in Table 2-3 are the maximum values attained by the respective uncertainties as they were propagated.

*The uncertainties assumed for the consider parameters and the data weights used are shown in Table 2-1.

Table 2-3(a). Results of Error Analysis Runs Using Simulated Trilateration and SST Data (Solving for one satellite state vector only)

Solve for GEOS-3 (target) only, consider 14 parameters

Data Span	Max. Uncertainties Due To Noise			Max. Uncertainties Due To Consider Parameters			Significant Consider Parameters
	H	L	C	H	L	C	
6-Hour	0.06	0.37	0.15	62.7	260.0	33.0	ATS Vector and Grav. Constant
12-Hour	0.04	0.18	0.05	61.9	429.1	118.9	ATS Vector and Grav. Constant

Solve for ATS-6 (relay) only, consider 14 parameters

Data Span	Max. Uncertainties Due To Noise			Max. Uncertainties Due To Consider Parameters			Significant Consider Parameters
	H	L	C	H	L	C	
6-Hour	0.31	0.48	0.52	2069	8718	34100	GEOS Vector and Grav. Constant
12-Hour	0.20	0.41	0.30	3966	24590	40560	GEOS Vector and Grav. Constant

Notes:

- 1) Units for radial (H), along-track (L), and cross-track (C) uncertainties are meters.
- 2) Data weights and consider parameter uncertainties are shown in Table 2-1.
- 3) The uncertainties have been propagated through the data span and the maximum values attained by each component are tabulated.

Table 2-3(b). Results of Error Analysis Runs Using
Simulated Trilateration and SST Data
(Solving for both satellite state vectors)

Solve for both GEOS-3 (target) and ATS-6 (relay), consider 8 parameters

ELEMENT	6-HOUR DATA SPAN			12-HOUR DATA SPAN		
	NOISE (at Epoch)	CONSIDER (at Epoch)	SIGNIFICANT CONSIDER PARAMETERS	NOISE (at Epoch)	CONSIDER (at Epoch)	SIGNIFICANT CONSIDER PARAMETERS
GEOS X (meters)	2.30	26.04	Grav. Constant	1.39	43.80	Grav. Constant, Range Bias
Y	2.07	22.01	Grav. Constant	1.31	35.97	Grav. Constant
Z	1.81	27.62	Grav. Constant, Rosman Lat.	0.95	25.03	Grav. Constant, Rosman Lat.
\dot{X} (cm/sec)	0.13	4.25	Grav. Constant	0.07	4.09	Grav. Constant, Range Bias
\dot{Y}	0.22	2.37	Rosman Lat., Rosman Ht.	0.12	2.69	Grav. Constant, Rosman Lat.
\dot{Z}	0.07	1.68	Grav. Constant	0.03	1.31	Grav. Constant
ATS X (meters)	16.88	125.0	Grav. Constant	10.42	265.0	Grav. Constant
Y	8.56	50.3	Grav. Constant, Range Bias	5.26	117.8	Grav. Constant, Range Bias
Z	7.35	211.1	Grav. Constant, Ros. Position	3.68	164.2	Grav. Constant, Ros. Position
\dot{X} (cm/sec)	0.06	0.19	Grav. Const., Rng Bias, Ros. Lat.	0.04	0.72	Grav. Constant, Range Bias
\dot{Y}	0.12	0.80	Grav. Constant	0.08	1.85	Grav. Constant
\dot{Z}	0.06	1.63	Grav. Constant, Rosman Lat.	0.03	1.34	Grav. Constant, Range Bias

Notes:

- 1) Data weights and consider parameter uncertainties are shown in Table 2-1.
- 2) Uncertainties due to noise and the consider parameters tabulated are those at epoch, which occurred approximately 40 minutes before the beginning of the data.

For runs in configuration (c), limitations in the NAPCOV program prevented the simultaneous rotation to HLC coordinates and propagation of two different state vectors; hence, the uncertainties for these runs are given in XYZ coordinates at epoch.

The following trends are evident in Table 2-3. As expected, when only the target satellite is being solved for, the uncertainties arising from noise decrease as the length of the data span increases, but those arising from the consider variables increase with the length of the data span (for extremely short spans of the order of a single pass, the uncertainties arising from both the noise and the consider parameters become very large, as shown in Reference 1).

When SST data are included in a solution for the ATS-6 state vector only, using fixed a priori values for the target satellite state vector, large errors may be introduced into the solution unless the measurement uncertainties used to weight the SST data are very large. This problem arises because discrepancies in the SST measurements, brought about by inaccuracies in the target satellite state vector or in dynamic parameters affecting the target satellite's orbit, will, if processed on an equal footing with direct tracking, produce large and unwanted corrections in the relay satellite's orbit. This applies particularly to the Doppler measurement, since the Doppler shift due to motion of a geosynchronous relay satellite is very small compared with that resulting from the motion of the target. This problem is reflected in the error analysis results in Table 2-3(a), in which the SST and trilateration data are given equal weights; the large uncertainties in the ATS-6 state vector arising from consider parameters are typical of this effect. If both satellite state vectors are adjusted, as in Table 2-3(b), the uncertainties in the solve-for parameters become tolerable. While the additional SST data, if properly weighted to reflect all the uncertainties affecting the target satellite orbit,

should, in theory, improve the solution, the correct weightings are sufficiently large and uncertain to suggest that SST data should be excluded when solving for the relay satellite only.

The major consider parameters are listed in the right-hand column of each table. The most prevalent of these are the coefficient of the spherically symmetric term in the geopotential (listed as "Grav. Constant" in the tables) and the state vector components not being solved for. The range bias term also becomes significant for the long data span when both state vectors are being solved for. The noise contributions to the solve-for uncertainties are all well below those of the consider parameters.

2.3 REAL GEOS-3 DATA

An error analysis study of ATS-6/GEOS-3 SST data recorded on April 27-28, 1975, was conducted in conjunction with the differential correction data processing of these data described in Section 3. The same observational data base was used in both sets of runs, so that the tracking schedules in the error analyses correspond to those in the differential correction. The data consist of:

- a) Three pairs of consecutive passes of SST relay data from GEOS-3 with an interval of approximately 10 hours between pairs (for convenience, these six passes are numbered "1" through "6" in the discussion to follow). Most of these data were Doppler type, with a few range type data points included in pass 3.
- b) ATS-6 coherent-mode tracking data from Rosman, with a small quantity of data relayed through a ground transponder at Santiago.
- c) ATS-6 tracking data from Mojave (only the range data were used).

The data separation for (a) and (b) was 10 seconds, and for (c) was 1 second.

The six passes of GEOS-3 data were studied in the following nine segments:

- Pass 1
- Pass 3
- Pass 5
- Passes 1-2
- Passes 3-4

Passes 5-6

Passes 1-4

Passes 3-6

Passes 1-6

Starting with a priori state vectors determined from the differential correction runs (described in Section 3), the data were processed by NAP for one iteration in the differential correction mode.

The normal matrix computed during the differential correction process and the orbit files generated by the integrator were passed to the NAP covariance analysis program (NAPCOV) to determine the contributions to solve-for uncertainties arising from the uncertainties in the consider parameters and to propagate these quantities in time.

Each span of data was used in three modes:

1. Solving for both the GEOS-3 and the ATS-6 state vectors (while considering uncertainties* in a number of dynamic and measurement parameters), using only the SST relay data
2. Solving for both the GEOS-3 and the ATS-6 state vectors (while considering fourteen uncertainties*), using both the SST relay data and the adjacent ATS-6 tracking data
3. Solving for the GEOS-3 state vector only, considering the ATS-6 state vector and other uncertainties*

*The uncertainties are shown in Table 2-4. The Mojave uncertainties are not used when solving for GEOS-3 only or when solving for both GEOS-3 and ATS-6 using only the SST relay data.

Table 2-4. Uncertainties Assumed for the Measurements
and for the Consider Parameters

A: Uncertainties in SST Data (Weighting Factors)

Range:	5×10^{-7} seconds = 75 meters (one-way)
Doppler:	2×10^{-6} seconds = 0.1 Hz (one-way)

B: Uncertainties in Consider Parameters

ATS-6 position:*	200 meters (each component)
ATS-6 velocity:*	0.465 cm/sec (X and Y components) 2.97 cm/sec (Z components)
Rosman station location:	10 meters (each component)
Rosman range bias:	10^{-7} sec = 15 meters (one-way)
Rosman Doppler bias:	0.5×10^{-7} sec
Mojave station location:	10 meters (each component)
Mojave range bias:	10^{-7} sec = 15 meters (one-way)
Solar pressure on ATS-6:	10%
C_{00} (coefficient of spherically symmetric component of gravitational field):	2×10^{-6}
C_{20} (coefficient of quadrupole term in gravitational field):	9.2×10^{-9}
C_{30} (3rd zonal coefficient in gravitational field):	1.125×10^{-8}
C_{40} (4th zonal coefficient in gravitational field):	3.0×10^{-8}

*The ATS-6 state vector uncertainties are based on the results of previous
error analysis studies of ATS-6 direct-tracking data.

Since NAPCOV was unable to propagate uncertainties in more than one state vector at a time, runs in modes 1 and 2 provide only the uncertainties at epoch, whereas in mode 3 the uncertainties were rotated to HLC coordinates and propagated through the data span. Since some of the consider parameters (e.g., the Mojave station coordinates) apply only to the ATS-6 tracking data, they contribute to the solve-for uncertainties only in mode 2.

The results of the runs for modes 1, 2, and 3 are shown in Tables 2-5, 2-6, and 2-7, respectively.

Table 2-5 does not contain results for single-pass runs, because a single pass of SST relay data by itself is insufficient to solve for both the GEOS-3 and the ATS-6 state vectors simultaneously. However, over a time span of two passes, the ATS-6 relay satellite position varies relative to the GEOS-3 orbital plane sufficiently to allow a solution to be obtained with the SST relay data. However, the uncertainties shown in Table 2-4 for the pairs of passes 1-2, 3-4, and 5-6 are large. Combining several adjacent passes of SST relay data, e.g., passes 1-4, 3-6, and 1-6, greatly reduces the large uncertainties due to noise, but affords no improvement to the uncertainties due to the consider parameters.

Table 2-5 shows the great advantage of using the adjacent ATS-6 tracking data in conjunction with the SST relay data. For the longer runs, e.g., passes 1-4, 3-6, and 1-6, the ATS-6 data reduces the uncertainties due to noise by a factor of about 10, and those due to consider parameters by a factor of about 20. The two-pass runs, e.g., 1-2, 3-4, and 5-6, show a similar reduction of the uncertainties due to both the noise and the consider parameters when the adjacent ATS-6 tracking data are included. The very large uncertainties in the two-pass data on run span 1-2 arise from the lack of Mojave data in this span. Thus, the geometrical advantage of having two different station positions was lost. The importance of the Mojave data is further demonstrated by the

Table 2-5 GEOS-3 (Target) and ATS-6 (Relay) State Vector Uncertainties
at Epoch Using Only SST Data

PASS	ERROR SOURCE	GEOS-3						ATS-6					
		X(meters)	Y	Z	\dot{X} (cm/sec)	\dot{Y}	\dot{Z}	X(meters)	Y	Z	\dot{X} (cm/sec)	\dot{Y}	\dot{Z}
1-2	Noise	15710	6173	2200	2016	1338	204	151070	23910	17190	192	1092	82.8
	Consider	1151	289.8	367.7	121.9	61.59	37.27	9778	1441	2955	13.36	71.37	7.156
1-2 (no range)	Noise	13330	1256	2964	1303	691	248	108170	18800	22550	138	797	109.9
	Consider	581.2	300.0	295.6	52.32	31.32	30.99	4157	699.7	2377	6.033	32.56	6.424
3-4	Noise	34230	37600	25670	14520	7543	2479	956000	159770	54570	1236	6770	3340
	Consider	1010	747.6	408.4	300.0	159.5	57.34	20300	3314	615.8	26.48	144.2	59.60
5-6	Noise	28760	10230	5430	2990	2111	486	232430	38530	35900	295	1695	210
	Consider	961.6	184.6	254.4	81.79	48.36	13.91	5915	1035	1892	7.18	43.88	12.23
1-4	Noise	273	104	39.0	38.0	23.8	4.60	2762	479	313	3.47	20.1	2.7
	Consider	866.9	250.1	33.52	95.20	63.02	5.93	7497	1245	359.2	9.11	54.72	2.25
3-6	Noise	369	142	55.7	41.4	29.1	7.53	3099	546	379	3.80	22.6	5.6
	Consider	1223	368.3	31.04	140.8	92.27	4.919	10830	1833	311.6	13.22	79.03	1.170
1-6	Noise	201	81.1	28.9	25.7	17.3	2.70	1930	334.7	222	2.4	14.0	1.4
	Consider	984.2	282.1	12.67	114.1	73.42	2.758	8807	1472	156.7	10.79	64.23	0.782

Notes:

- 1) Results for the single passes 1, 3, and 5 are not included in this table since a single pass of SST relay data by itself is insufficient to solve for both the GEOS and the ATS state vectors simultaneously.
- 2) The consider parameter uncertainties are those given in Table 2-4, excluding the ATS-6 and the Mojave uncertainties.

Table 2-6. GEOS-3 (Target) and ATS-6 (Relay) State Vector Uncertainties
at Epoch Using SST Data and ATS-6 Tracking Data

PASS	ERROR SOURCE	GEOS-3						ATS-6					
		X(meters)	Y	Z	\dot{X} (cm/sec)	\dot{Y}	\dot{Z}	X(meters)	Y	Z	\dot{X} (cm/sec)	\dot{Y}	\dot{Z}
1	Noise												
	Consider												
3	Noise	243500	258800	171300	518.1	22850	33850	216.2	92.15	143.9	0.874	1.587	1.219
	Consider	849.2	884.2	580.3	5.22	78.22	116.5	322.0	70.96	105.6	0.554	2.297	0.607
5	Noise	1550	2422	1700	58.98	219.0	257.8	238.9	27.02	198.3	0.338	1.562	0.755
	Consider	186.2	272.6	195.5	5.21	24.35	30.64	387.9	62.59	58.68	0.733	2.785	1.007
1-2	Noise	123.2	91.11	94.37	7.23	5.41	7.51	441.6	56.80	596.2	0.834	3.359	5.430
	Consider	185.2	44.53	44.40	20.49	10.67	6.35	1545	205.2	390.8	1.916	11.31	1.937
3-4	Noise	64.30	65.45	41.28	1.12	5.90	8.36	72.70	18.31	74.75	0.138	0.509	0.521
	Consider	194.0	173.1	99.66	4.07	15.46	23.71	326.0	64.54	139.6	0.588	2.344	0.245
5-6	Noise	37.73	44.99	30.53	1.19	4.09	5.10	92.32	14.35	80.67	0.117	0.652	0.583
	Consider	99.18	130.6	99.18	3.78	12.19	14.81	422.8	67.50	91.80	0.772	3.03	0.814
1-4	Noise	9.23	9.32	7.53	0.944	0.956	0.902	61.86	12.98	62.89	0.069	0.413	0.443
	Consider	30.02	15.69	7.92	3.39	2.74	0.994	268.7	57.14	67.56	0.377	1.95	0.251
3-6	Noise	9.09	7.85	6.02	0.506	0.680	0.923	33.89	6.95	41.55	0.046	0.246	0.326
	Consider	35.53	21.16	24.31	3.037	2.79	1.02	307.7	50.12	34.60	0.646	2.16	0.898
1-6	Noise	6.83	5.26	4.31	0.493	0.466	0.619	32.95	6.64	38.73	0.042	0.241	0.291
	Consider	32.37	11.47	9.40	2.96	2.43	1.02	256.7	54.93	37.30	0.443	1.88	0.514

NOTES: 1) The absence of Mojave data in pass 1 makes it impossible to solve for both the GEOS-3 and the ATS-6 state vectors simultaneously.

2) The fourteen consider parameter uncertainties are shown in Table 2-4.

Table 2-7. GEOS-3 (Target) State Vector Uncertainties, Using
SST Data and Considering ATS-6 (Relay) State
Vector Uncertainties

PASS	Max Uncertainties Due To Noise			Max Uncertainties Due To Consider Parameters			Significant Consider Parameters
	H	L	C	H	L	C	
1	221.8	4260	45.8	415.0	12120	523.4	ATS-6 state vector, grav. coeff. C_{00}
3	13014	194940	245590	99.4	2320	1871	ATS-6 state vector, grav. coeff. C_{00} and C_{40}
5	59.3	60200	46.3	124.1	160700	981.0	ATS-6 state vector, grav. coeff. C_{00} , ATS-6 solar press.
1-2	1.82	12.4	6.97	54.05	136.7	118.9	ATS-6 state vector, grav. coeff. C_{00}
1-2 (no range)	8.17	117.3	4.94	373.8	2013	83.56	ATS-6 state vector, grav. coeff. C_{00}
3-4	3.03	1172	29.0	55.67	25860	294.0	ATS-6 state vector, grav. coeff. C_{00}
5-6	2.74	1945	4.91	82.73	76780	594.6	ATS-6 state vector, grav. coeff. C_{00}
1-4	0.797	2.25	2.68	86.47	2958	175.0	grav. coeff. C_{00} , ATS-6 state vector
3-6	0.825	4.74	1.87	72.21	624.5	542.8	ATS-6 state vector, grav. coeff. C_{00}
1-6	0.534	1.60	1.32	45.31	230.4	403.3	ATS-6 state vector, grav. coeff. C_{00}

Notes:

- 1) The maximum values attained by the uncertainties when propagated through the data span are tabulated.
- 2) The consider parameter uncertainties are those given in Table 2-4, excluding the Mojave uncertainties.
- 3) Units for radial (H), along-track (L), and cross-track (C) uncertainties are meters.

the results for pass 1, where, lacking a Mojave component, the data were insufficient to solve for both the GEOS-3 and the ATS-6 state vectors simultaneously.

The GEOS-3 uncertainties in pass 3 are much larger than those in pass 5 since approximately two-thirds of the SST data points in pass 3 were bad and were eliminated by the editing process. The scarcity of the resulting pass 3 data is also reflected in the large uncertainties for the two-pass data span on run 3-4 shown in Table 2-4. Due to the sparseness of the SST data in pass 3, the results shown for run 3-4 in Table 2-4 are based on little more than one pass of SST data, which is insufficient to solve for both the GEOS-3 and the ATS-6 state vectors simultaneously.

Table 2-6 contains the results obtained from error analysis runs when solving for the GEOS-3 elements only. The noise and consider uncertainties computed at epoch in each of these runs were rotated into HLC coordinates and propagated through the data span; the values tabulated are the maximum values obtained by the uncertainties within the span of propagation.

SECTION 3 - DIFFERENTIAL CORRECTION PROCESSING
OF REAL SST DATA

The SST data of April 27-28 were used to obtain values for the GEOS-3 and ATS-6 state vectors. Differential correction runs were made using NAP on the nine segments of the data shown on pages 2-11 and 2-12. In the first run, all the ATS-6 direct-tracking data in passes 1-6 were used to solve for the ATS-6 state vector only. The resulting state vector* and associated uncertainties were:

ATS X = $0.7091651968036083 \times 10^7$ meters	$\sigma_x = 170.5$ meters
ATS Y = $-0.4156110240838270 \times 10^8$	$\sigma_y = 31.8$
ATS Z = $0.2553856432432547 \times 10^6$	$\sigma_z = 162.0$
ATS \dot{X} = $0.3030356912466290 \times 10^6$ cm/sec	$\sigma_{\dot{x}} = 0.27$ cm/sec
ATS \dot{Y} = $0.5183989881342083 \times 10^5$	$\sigma_{\dot{y}} = 1.20$
ATS \dot{Z} = $0.5191434084728750 \times 10^4$	$\sigma_{\dot{z}} = 1.22$

With the ATS-6 state vector held constant at this value, the nine segments of data were processed by NAP in the differential correction mode to solve for GEOS-3 only. The results of this study are shown in Table 3-1. In order to facilitate comparisons between the solutions obtained, these results are specified relative to the GEOS-3 state vector obtained from the segment containing all six passes of GEOS-3 data, i.e., run 1-6 in Table 3-1. The state vector deviations in Table 3-1 are thus simple mathematical differences between the several solutions obtained and the following reference state vector* obtained in run 1-6:

GEOS X = $-0.12665752957 \times 10^7$ meters
GEOS Y = $-0.46002468881 \times 10^7$
GEOS Z = $0.54157448935 \times 10^7$

*The epoch is $10^h 36^m$ UT on April 27.

Table 3-1. GEOS-3 (Target) State Vector Deviations and Uncertainties Using SST Data

PASS	X(meters)		Y		Z		\dot{X} (cm/sec)		\dot{Y}		\dot{Z}	
	Deviation	σ	Deviation	σ	Deviation	σ	Deviation	σ	Deviation	σ	Deviation	σ
1	217.4	1.96	-62.1	1.90	-80.7	1.44	24.526	0.1988	-3.630	0.1053	38.901	0.1629
3	121.0	7.80	-47.0	7.14	-91.3	7.69	24.812	0.2053	-3.624	0.1085	38.933	0.1673
5	209.9	2.07	-45.5	1.95	-62.5	1.52	24.460	0.1990	-3.716	0.1062	38.834	0.1639
1-2	76.0	2.64	-109.8	2.62	-96.1	1.80	-11.805	0.6364	-14.779	0.2301	15.520	0.3556
3-4	160.4	63.33	-78.3	64.46	-92.8	40.15	39.679	0.3268	1.127	5.8030	43.690	8.2865
5-6	-2470.5	24.95	3924.4	37.69	2777.2	25.63	66.628	0.5684	339.447	3.3246	-425.041	4.1787
1-4	227.2	1.98	-91.2	1.39	-49.0	0.89	28.103	0.1832	-5.994	0.0789	37.295	0.2487
3-6	-303.0	2.25	641.4	3.57	468.5	2.54	29.848	0.1865	55.648	0.2910	-50.849	0.3037
1-6	0.0	1.28	0.0	1.18	0.0	0.73	0.0	0.0984	0.0	0.0690	0.0	0.1392

Notes:

- 1) The state vector solution obtained for passes 1-6 (shown on page 3-1) is used as the reference point for this table and all other solutions are expressed as deviations from that solution.
- 2) Note that these runs solved only for the GEOS-3 state vector. The ATS-6 state vector was held fixed at the values listed on page 3-1. No consider variables were included.

$$\text{GEOS } \dot{X} = -0.34431286721 \times 10^6 \text{ (cm/sec)}$$

$$\text{GEOS } \dot{Y} = 0.53952690741 \times 10^6$$

$$\text{GEOS } \dot{Z} = 0.37753037804 \times 10^6$$

It should be noted that the GEOS-3 reference state vector is the final solution obtained on one of the data spans, not the a priori value used to process the data. The ATS-6 reference state vector was obtained by processing only the ATS-6 tracking data, and was subsequently used as an a priori value for all the SST data processing. The a priori values used for the GEOS-3 state vector were adjusted to obtain convergence for a given data span. In many cases it required two or three runs, adjusting both the GEOS-3 a priori vector and the data edit criteria, in order to obtain a convergence.

Although the six solutions which do not include pass 6 are reasonably consistent, the data on pass 6 appear to have a strong perturbing effect on the solutions. These are real data and the reason for this perturbation is unknown. Since the fit to the data on the ATS-only solution does not become appreciably worse at the end of the data span, an ATS-6 maneuver is not a likely explanation. It is more probable that during the final pass a perturbation was introduced into either the GEOS-3 trajectory or the phase-locked-loop mode of the tracking system.

The comparatively large computed uncertainties in runs containing pass 3 reflect the fact that two-thirds of the pass 3 data were edited and not included in the solutions.

An attempt was made to do differential correction runs solving for both the GEOS-3 and the ATS-6 state vectors simultaneously. The various multiple-pass data segments were used in these runs. In only one of these differential correction runs, the one utilizing the data in passes 1-4, did the differential correction process converge to a solution for GEOS-3 and ATS-6. The results, shown in Table 3-2, are expressed as deviations about reference state

Table 3-2. GEOS-3 (Target) and ATS-6 (Relay) State Vector Deviations and
Uncertainties Using SST Data

PASS	X(meters)		Y		Z		\dot{X} (cm/sec)		\dot{Y}		\dot{Z}	
	Deviation	σ	Deviation	σ	Deviation	σ	Deviation	σ	Deviation	σ	Deviation	σ
1-4	GEOS	1642.4	37.37	-49.6	26.67	253.9	25.70	84.11	3.153	-11.55	2.207	3.006
	ATS	1013.6	197.78	46.2	33.65	-2214.3	208.99	-0.51	0.264	12.82	1.444	1.720

The state vector solutions obtained from passes 1-6 when solving for ATS-6 only and for GEOS-3 only (see page 3-1) are used as the reference points for this table, and the solutions are expressed as deviations from those solutions.

vectors. The GEOS-3 reference state vector is the same as was used in Table 3-1. The ATS-6 reference state vector was chosen to be the ATS-only solution shown on page 3-1. The large corrections (see Table 3-2) necessary to this ATS-only solution when processing SST data only indicate an inconsistency between the ATS-6 tracking data and the SST data.

APPENDIX A - MATHEMATICAL METHOD USED IN ERROR ANALYSES

The notation in this section is taken from Chapter 8 of Reference 2. In particular, the following are defined:

x_0 = a priori value of vector of solve-for parameters

z_0 = a priori value of vector of consider parameters

W = diagonal measurement weighting matrix

$f(x, z)$ = measurement modeling algorithm as a function of solve-for and consider parameters

$F = \left. \frac{\partial f}{\partial x} \right|_{(x_0, z_0)} = \text{partial derivative matrix with respect to solve-for parameters}$

$E = \left. \frac{\partial f}{\partial z} \right|_{(x_0, z_0)} = \text{partial derivative matrix with respect to consider parameters}$

$P_{\Delta x_0}$ = a priori (Bayesian) covariance matrix for solve-for parameters

$P_{\Delta z_0}$ = a priori covariance matrix for consider parameters

The method used by NAP and NAPCOV ignores the correlation matrix between solve-for and consider parameters, and in all studies reported in this document the Bayesian term $P_{\Delta x_0}$ was also omitted. With these simplifications, Equation (8-39) of Reference 2 reduces to:

$$P_{\Delta x} = \psi \left[F^T W E P_{\Delta z_0} E^T W F + \psi^{-1} \right] \psi^T$$

where $\psi \equiv (F^T W F)^{-1}$

$$\therefore P_{\Delta x} = \psi F^T W E P_{\Delta z_0} E^T W F \psi^T + \psi$$

The first term of this expression gives the covariance of the solve-for parameters arising from the consider parameter covariance $P_{\Delta z}^o$; the second term reflects only the data noise. The square roots of the diagonal elements of these matrices provide the uncertainties in solve-for parameters due to consider parameters and noise, which are listed in the body of this report. Replacing the complete diagonal matrix $P_{\Delta z}^o$ by a matrix containing a nonzero element for only one consider parameter allows the effects of individual consider parameters to be estimated; in this way the major contributors to the overall uncertainties are identified.

REFERENCES

1. Computer Sciences Corporation, CSC/TM-75/6110, Satellite to Satellite Tracking Error Analysis Studies, C. L. Ayres, G. Rosenblatt, G. P. Spears, and W. E. Wagner, June 1975
2. Goddard Space Flight Center, (in publication), Goddard Trajectory Determination System Mathematical Specifications, J. O. Cappellari Jr. and C. E. Velez, October 1975